

Evidence for Strong Mixing Between the LC and MLCT Excited States in Some Heteroleptic Iridium (III) Complexes

Jayaraman Jayabharathi · Venugopal Thanikachalam · Natesan Srinivasan · Marimuthu Venkatesh Perumal

Received: 1 November 2010 / Accepted: 12 January 2011 / Published online: 28 January 2011
© Springer Science+Business Media, LLC 2011

Abstract The synthesis, structure and photophysical properties of series of new luminescent cyclometalated Iridium (III) complexes are reported. The cyclometalated ligand used here is 2-aryl imidazole and the auxiliary ligand is acetyl acetone (acac). The crystal structure of the complex (*dmdpi*)₂Ir(acac) (5) show that the Iridium(III) ion resides in a distorted octahedral environment. All complexes exhibit bright photoluminescence (PL) at room temperature and (*fpdmdmpi*)₂Ir(acac) 4 has a high solution PL quantum efficiency of 0.56. The role played by electron releasing and electron withdrawing substituents of the 2-arylimidazole ligands towards the stability of HOMO and how the substituent influences the luminescent behaviour are discussed. Furthermore those substituents have effect on the contribution to mixing between ³(π-π*) and ³(MLCT) for the lowest excited states.

Keywords Mixed LC and MLCT excited states · Spin-orbit coupling · Colour tuning · DFT calculation · HOMO-LUMO orbitals · Transphobia

Introduction

Organometallic complexes possessing a heavy transition-metal element are crucial for the fabrication of phosphorescent organic light-emitting devices (OLEDs) [1–7]. The strong spin-orbit coupling effectively promotes intersystem crossing as well as enhances the subsequent emissive decay

from the triplet excited state to the ground state, facilitating strong phosphorescence by harvesting both singlet and triplet excitons. Because an internal quantum efficiency as high as 100% can theoretically be achieved, these heavy-metal containing emitters are superior to their fluorescent counterparts in OLED applications [1, 8]. Iridium-based emitters are considered to be the seminal generation of phosphorescence emitters due to their high stability, high photoluminescence (PL) efficiency and relatively short excited state lifetime. A major effort in the research of phosphorescent materials is the designing new cyclometalated ligands or auxiliary ligands to tune the emission colour of the resulting complexes [9–11]. The research group by Thompson et al., have synthesized and reported a neutral emissive cyclometalated Iridium (III) [12, 13] and platinum(II) [14] complexes and used them in the fabrication of OLEDs as a phosphorescent dopant successively. A series of Iridium (III) complexes with fluorinated 2-arylpyridines have been synthesized and characterized and showed that the emissive colours of the materials can be finely tuned by systematic control of the nature and position of the substituent of the ligands [15]. Furthermore a series of Iridium(III) complexes with substituted 2-phenylbenzothiazoles as the cyclometalated ligands have also synthesized and characterized and showed that the electroluminescent (EL) efficiency and emissive colours of OLEDs based on these Iridium(III) complexes could be finely tuned by suitable modification of the substituent on ligands [16]. The classification into ligand centered (LC) T-T* and metal to ligand charge-transfer (MLCT) transitions is normally made on the basis of luminescence lifetimes and band shapes, whereas the active ligand in mixed-ligand complexes is identified by electrochemical measurements. Quite often room-temperature solution spectra are sufficient for such a classification, but in some cases, especially when the LC and MLCT excited

J. Jayabharathi (✉) · V. Thanikachalam · N. Srinivasan · M. V. Perumal
Department of Chemistry, Annamalai University,
Annamalainagar 608002 Tamilnadu, India
e-mail: jtchalam2005@yahoo.co.in

states lie close to each other, solid-state spectroscopic methods at cryogenic temperatures have to be applied. These research activities inspired us to initiate a systematic study [17–20] on the luminescent behaviour of new cyclometalated novel Iridium (III) complexes by both experimentally and also theoretically and we have exploited that the substantial mixing between these states of lowest excited LC and MLCT states in the title compound and that there is.

Experimental

Materials and Methods

Iridium(III) trichloride trihydrate ($\text{IrCl}_3 \cdot 3\text{H}_2\text{O}$, Sigma-Aldrich Ltd.), 2-ethoxyethanol ($\text{H}_5\text{C}_2\text{OC}_2\text{H}_4\text{OH}$, S.D. fine) and all the other reagents used without further purification.

Optical Measurements and Compositions Analysis

The ultraviolet-visible (UV-vis) spectra of the phosphorescent Ir(III) complexes were measured in an UV-vis spectrophotometer (Perkin Elmer Lambda 35) and corrected for background absorption due to solvent. Photoluminescence (PL) spectra were recorded on a (Perkin Elmer LS55) fluorescence spectrometer. The solid-state emission spectra were recorded on fluoromax 2 (ISA SPEX) xenon-Arc lamp as a source. NMR spectra were recorded on a Bruker 400 MHz NMR spectrometer. MS spectra (EI and FAB) were recorded on a Varian Saturn 2200 GCMS spectrometer. Cyclic voltammetry (CV) analyses were performed by using CHI 630A potentiostap electrochemical analyzer. Measurements of oxidation and reduction were undertaken using 0.1 M tetra(n-butyl)ammonium-hexafluorophosphate as the supporting electrolyte, at scan rate of 0.1 Vs^{-1} . The potentials were measured against an Ag/Ag^+ (AgCl) reference electrode using ferrocene/ferrocenium ($\text{CP}_2\text{Fe}/\text{CP}_2\text{Fe}^+$) as the internal standard. The onset potentials were determined from the intersection of two tangents drawn at the rising current and background current of the cyclic voltammogram.

General Procedure for the Synthesis of Ligands

The various substituted 2-arylimidazole ligands were prepared from an unusual four components assembling of Butan-2,3-dione, ammonium acetate, substituted aryl amine and an substituted arylaldehyde as shown in Scheme 1 [21].

1. 4,5-dimethyl-2-phenyl-1-*p*-tolyl-1H-imidazole (dmpti)

Yield: 48%. ^1H NMR (400 MHz, CDCl_3): δ 2.42 (s, 3H), 2.31 (s, 3H), 2.02 (s, 3H), 7.02–7.36 (aromatic protons). ^{13}C NMR (100 MHz, CDCl_3): δ 9.57, 12.76, 21.19, 125.45, 127.54, 127.63, 127.97, 128.01, 130.11, 130.92, 133.41,

135.34, 138.37, 145.15. Anal. calcd. for $\text{C}_{18}\text{H}_{18}\text{N}_2$: C, 82.41; H, 6.92; N, 10.68. Found: C, 82.12; H, 6.02; N, 10.08. MS: m/z 262.15, calcd. 262.00.

2. 2-(4-fluorophenyl)-4,5-dimethyl-1-*p*-tolyl-1H-imidazole (fpdmpti)

Yield: 40%. ^1H NMR (400 MHz, CDCl_3): δ 2.01 (s, 3H), 2.29 (s, 3H), 2.43 (s, 3H), 6.87–7.34 (aromatic protons). ^{13}C NMR (100 MHz, CDCl_3): δ 9.53, 12.69, 21.18, 114.92, 115.10, 125.44, 127.16, 129.89, 130.20, 133.35, 135.13, 138.57, 144.28, 161.26, 163.23. Anal. calcd. for $\text{C}_{18}\text{H}_{17}\text{N}_2\text{F}$: C, 77.12; H, 6.11; N, 9.99. Found: C, 76.24; H, 5.98; N, 8.99. MS: m/z 280.00, calcd. 280.14.

3. 4,5-dimethyl-1-(3,5-dimethylphenyl)-2-phenyl-1H-imidazole (dmdmppi)

Yield: 45%. ^1H NMR (400 MHz, CDCl_3): δ 1.98 (s, 3H), 2.27 (s, 3H), 2.29 (s, 6H), 6.77–7.36 (aromatic protons). ^{13}C NMR (100 MHz, CDCl_3): δ 9.65, 12.77, 21.27, 125.54, 125.59, 127.59, 127.97, 128.03, 130.02, 130.07, 133.53, 137.88, 139.33, 144.98. Anal. calcd. for $\text{C}_{19}\text{H}_{20}\text{N}_2$: C, 82.57; H, 7.29; N, 10.14. Found: C, 82.01; H, 6.89; N, 9.12. MS: m/z 276.00, calcd. 276.16.

4. 2-(4-fluorophenyl)-4,5-dimethyl-1-(3,5-dimethylphenyl)-1H-imidazole (fpdmdmipi)

Yield: 45%. ^1H NMR (400 MHz, CDCl_3): δ 1.99 (s, 3H), 2.27 (s, 3H), 2.31 (s, 6H), 6.77–7.34 (aromatic protons). ^{13}C NMR (100 MHz, CDCl_3): δ 9.5, 12.69, 21.15, 114.81–163.41(aromatic carbons). Anal. calcd. for $\text{C}_{19}\text{H}_{19}\text{N}_2\text{F}$: C, 77.52; H, 6.51; N, 9.52. Found: C, 77.01; H, 6.02; N, 9.21. MS: 294.00, calcd. 294.15.

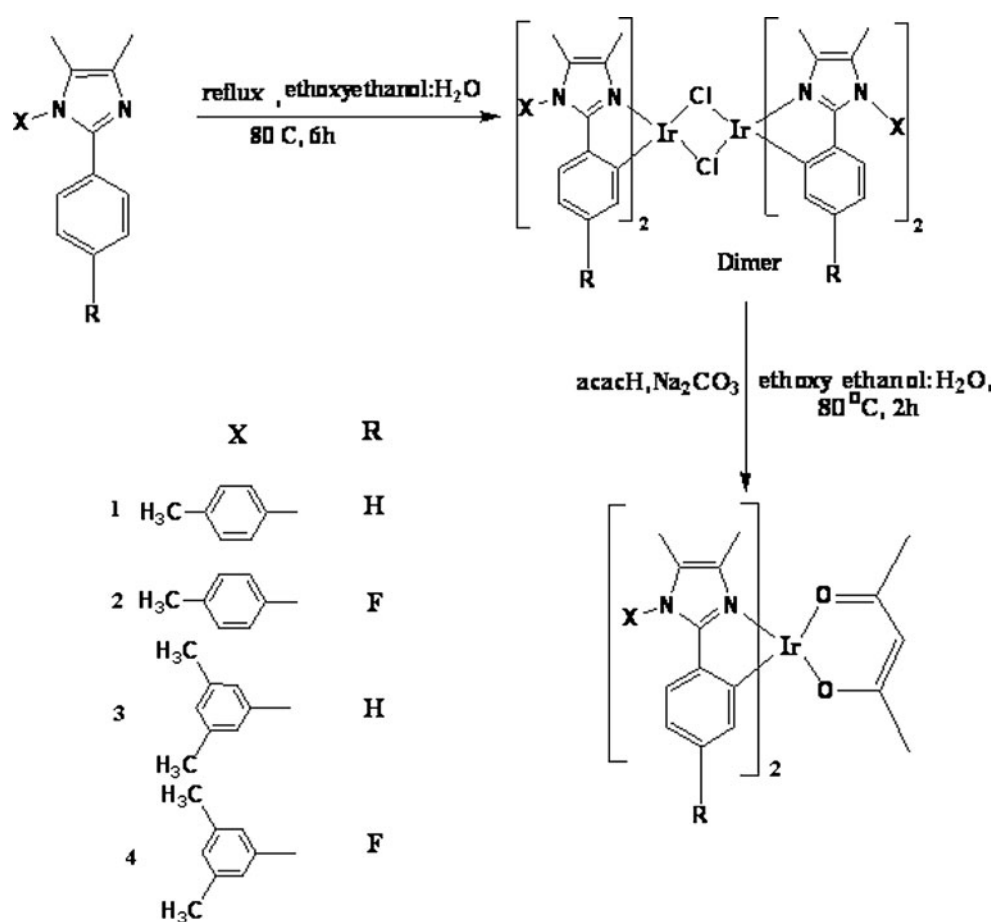
General Procedure for the Synthesis of Iridium Complexes (1–4)

The 2-aryl imidazole based cyclometalated iridium complexes **1–4** were readily synthesized from $\text{IrCl}_3 \cdot 3\text{H}_2\text{O}$ and the 2-aryl imidazole ligands to give the corresponding dimeric species via the Nonoyama route [22] followed by the treatment with acetylacetone in the presence of K_2CO_3 as shown in Scheme 1. These complexes are purified by column chromatography using hexane-ethyl acetate as the eluent.

1. Iridium(III)bis(4,5-dimethyl-1-(*p*-methylphenyl)-2-phenyl-1H-imidazolato-N,C_{2'})(acetyl acetonate) ($\text{Ir}(\text{dmpti})_2(\text{acac})$), 1

Yield: 55%. ^1H NMR (400 MHz, CDCl_3): δ 1.26 (s,2H), 1.54 (s, 3H), 1.76 (s, 3H), 2.00 (s, 3H), 2.17 (s,3H), 2.20 (s, 3H), 2.49 (s,6H), 5.27 (s, 1H), 6.13 (dd,1H, $J=1.0,9.5$ Hz), 6.36 (dd,1H, $J=4.2,10.53$ Hz), 6.48 (dd,2H, $J=1.12,7.6$ Hz), 6.52 (dd,2H, $J=1.32,7.08$ Hz), 7.00 (s,1H), 7.24 (dd,1H,

Scheme 1 Synthesis of ligands and Iridium complexes ($C^N_2Ir(acac)$) 1–4



$J=3.00, 7.00$ Hz), 7.31 (d,1H, $J=2.5$ Hz), 7.33 (d,3H, $J=2.5$ Hz), 7.34 (dd,3H, $J=5.5, 7.5$ Hz), 7.52 (s,1H). ^{13}C NMR (100 MHz, $CDCl_3$): δ 9.34, 14.10, 15.16, 21.37, 22.68, 27.09, 29.69, 119.94, 127.97, 129.50, 130.58, 133.86, 182.10. Anal. calcd. for $C_{41}H_{41}IrN_4O_2$: C, 60.50; H, 5.08; N, 6.88. Found: C, 59.86; H, 4.35; N, 6.01. MS: m/z 814.00, calcd. 814.29.

2. Iridium(III)bis(4,5-dimethyl-1-(*p*-methylphenyl)-2-fluorophenyl-1H-imidazolato-N,C2')(acetyl acetonate) ($Ir(fpdmnti)_2(acac)$), 2

Yield: 62%. 1H NMR (400 MHz, $CDCl_3$): δ 1.26 (s,3H), 1.56 (s, 3H), 1.78 (s, 3H), 1.99 (s, 6H), 2.18 (s, 3H), 2.49 (s, 6H), 5.30 (s,1H), 6.08 (s,1H), 6.10 (d,2H, $J=2.00$ Hz), 7.26 (s,2H); –7.36 (m,8H). ^{13}C NMR (100 MHz, $CDCl_3$): δ 9.29, 10.41, 21.39, 27.15, 28.34, 29.71 101.02, 102.10, 120.26, 122.50, 122.92, 128.11, 130.59, 133.35, 182.60, 184.25,. Anal. calcd. for $C_{41}H_{39}IrN_4O_2$: C, 57.93; H, 4.62; N, 6.59. Found: C, 56.89; H, 4.72; N, 5.01. MS: m/z 850.00, calcd. 850.27.

3. Iridium(III)bis(4,5-dimethyl-1-(3,5-di-methylphenyl)-2-phenyl-1H-imidazolato-N,C2')(acetyl acetonate) ($Ir(dmdmppi)_2(acac)$), 3

Yield: 62%. 1H NMR (400 MHz, $CDCl_3$): δ 1.65 (s, 6H), 1.79 (s, 6H), 2.04 (s, 6H), 2.23(s, 6H), 2.39 (s, 6H), 2.43 (s, 6H), 5.30 (s,1H), 6.17 (d,2H, $J=7.5$ Hz), 6.40 (d,2H, $J=7.23$ Hz), 6.51(d,2H, $J=7.00$ Hz), 6.57 (d,4H, $J=7.50$ Hz), 6.99 (s,2H), 7.09 (s,2H), 7.19 (s,2H). ^{13}C NMR (100 MHz, $CDCl_3$): δ 9.35, 10.47, 21.18, 28.27, 119.42, 121.70, 123.16, 125.91, 126.54, 130.97, 132.38, 134.09, 136.52, 137.29, 139.59, 144.70, 156.78, 183.99. Anal. calcd. for $C_{43}H_{45}IrN_4O_2$: C, 61.33; H 5.39; N, 6.65. Found: C, 61.00; H, 4.72; N, 5.01. MS: m/z 842.00, calcd 842.32.

4. Iridium(III)bis(4,5-dimethyl-1-(3,5-di-methylphenyl)-2-fluorophenyl-1H-imidazolato-N,C2')(acetyl acetonate) ($Ir(fpdmmpf)_2(acac)$), 4

Yield: 62%. 1H NMR (400 MHz, $CDCl_3$): δ 1.82 (s, 6H), 2.04 (s, 6H), 2.21 (s, 6H), 2.41 (s, 6H), 2.43 (s, 6H), 5.33 (s,1H), 6.13(t, 6H, $J=4.75$ Hz), 7.00(s,1H), 7.06 (s, 2H), 7.20 (s,1H). ^{13}C NMR (100 MHz, $CDCl_3$): δ 9.33, 10.36, 21.19, 28.33, 100.85, 106.25, 106.43, 120.01, 122.84, 123.30, 125.83, 131.16, 132.12, 133.38, 136.24, 139.73, 148.11, 156.03, 160.39, 162.37, 184.19. Anal. calcd. for $C_{43}H_{43}IrN_4O_2$: C, 58.82; H 4.94; N, 6.38. Found: C, 58.80; H, 4.72; N, 5.01. MS: m/z 878.00, calcd 878.30.

Theoretical Calculations

All calculations were performed using density functional theory (DFT) as implemented in the Gaussian 03 program [23]. The geometry optimization was carried out by B3LYP level using LANL2Z basis set [24].

Results and Discussion

Photophysical Properties

In order for these iridium (III) complexes to be useful as phosphors EL devices, strong spin-orbit coupling must be present to efficiently mix the singlet and triplet excited states. Clear evidences for mixing of the singlet and triplet excited states are seen in both the absorption (Fig. 1) and emission spectra (Fig. 2) of these complexes. Absorption and emission spectra were measured in various solvents at 298 K for complexes **1–4** and the pertinent data are summarized in Table 1. All the absorption spectra of these complexes display intense multiple absorption bands appearing in ultraviolet part of the spectrum between 250 and 425 nm. The measured energies and extinction coefficients are comparable to the free 2-aryl imidazole ligands. Hereby, these features are assigned to the spin-allowed intra ligand π - π^* transition of the imidazole ligands. Both singlet MLCT (1 MLCT) and triplet MLCT (3 MLCT) bands are typically observed for these complexes in all solvents. For example, $[\text{Ir}(\text{dmpti})_2(\text{acac})]$ (**1**), shows weak and broad absorption bands in the wavelength region 328 and 380 nm in dichloromethane at 298 K. According to the previous papers [12, 25], these weak bands located at long wavelengths have been assigned to the MLCT transitions of Iridium complexes. Thus, the broad absorption shoulders at 328 and 383 nm observed for $[\text{Ir}(\text{dmpti})_2(\text{acac})]$ (**1**), are likely to be ascribed to the 1 MLCT [$d\ \pi(\text{Ir}) \rightarrow \pi$ (ligand)] and 3 MLCT [$d\ \pi(\text{Ir}) \rightarrow \pi^*(\text{ligand})$], respectively. The intensity of the 3 MLCT transition is close to that of 1 MLCT, suggesting that the 3 MLCT transition is strongly allowed by an effective mixing of singlet-triplet with higher lying spin-allowed transitions on the cyclo-metatalated ligands [12]. This mixing is facilitated by the strong spin-orbit coupling of the iridium centre. In analogy, the weak absorption bands of $[\text{Ir}(\text{fpdmti})_2(\text{acac})]$ (**2**), at 337 and 376 nm are assumed to the 1 MLCT and 3 MLCT transitions, respectively. The broad and weak absorption band of $[\text{Ir}(\text{dmdmppi})_2(\text{acac})]$ (**3**) in the range of 355 and 415 nm appear to be the 1 MLCT and 3 MLCT transition and for $[\text{Ir}(\text{fpdmdmpti})_2(\text{acac})]$ (**4**) the weak absorption bands are at 376 and 408 nm. The similarity of the 3 MLCT energies for these complexes is unsurprising, since these complexes have similar 3 MLCT states involving the same fragment of

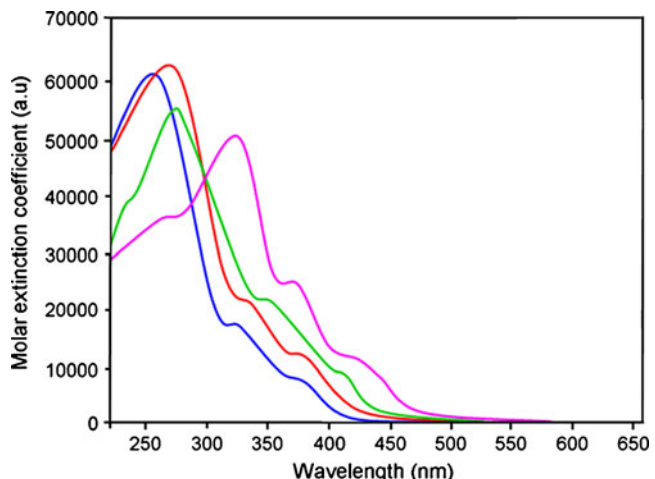


Fig. 1 The UV-vis absorption spectra of the complexes **1–4** in CH_2Cl_2

the 2-arylimidazole ligand. All these complexes show similar structural features in their emission spectra (Table 1), with emission maximum 505, 507, 510 and 514 nm respectively, in dichloromethane whereas in comparison with the complexes **1** and **3**, the emission spectra of **2** and **4** are broad. The emission spectra of complexes **1** and **2** are slightly blue-shifted in comparison with that of complexes **3** and **4**. $[\text{Ir}(\text{dmpti})_2(\text{acac})]$ (**1**) is blue shifted (5 nm) in comparison with that of $[\text{Ir}(\text{dmdmppi})_2(\text{acac})]$ (**3**). Similarly, complex **2** is blue-shifted (7 nm) in comparison with that of **4**, which is the result of the introduction of electron withdrawing fluorine substituent into the phenyl ring attached to C(2) carbon of the imidazole ring in complexes **2** and **4**. The photophysical studies of these complexes demonstrate that the electron releasing substituent increases the absorption and emission energies of complexes by stabilizing the HOMO, leaving the LUMO largely unchanged. Besides increasing the emission energy, the lower HOMO energies increase the energy separation between the 1 MLCT and 3 LC states, which in turn modified the excited state properties of the iridium complexes.

The frontier orbital components are obtained from the DFT calculations. The atomic orbital contributions for each complex, expressed in percentage, are given in Table 2. Percentage contributions were calculated from Eq. 1, where n is the atomic orbital coefficient and $\sum n^2$ is the sum of the squares of all atomic orbital coefficients in a specific molecular orbital [26].

$$\left[\frac{n^2}{\sum n^2} \right] \times 100 = \% \text{ contribution} \quad (1)$$

Each complex is divided into three parts namely, the metal iridium, 2-arylimidazole ligand and auxiliary ligand acetylacetone. The percentage contribution of each part is the sum of

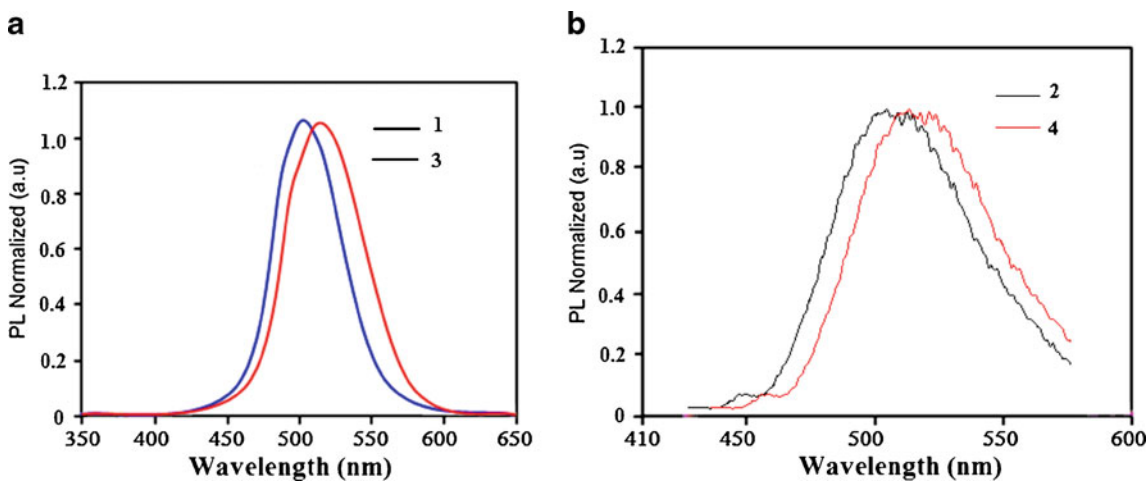


Fig. 2 **a** The photoluminescence emission spectra of the complexes **1** and **3** in CH_2Cl_2 and **b** the photoluminescence emission spectra of the complexes **2** and **4** in CH_2Cl_2

the atomic orbital coefficient square (Table 2). In general, for these complexes, their occupied orbitals (HOMO-1 and HOMO) compositions primarily localize on the ligand, admix with some contributions from the auxiliary ligand to metal iridium. In the case of fluoro substituted complexes **2** and **4**, the contributions of metal iridium and auxiliary ligand to the HOMO are decreasing. Besides, the two unoccupied orbitals (LUMO and LUMO+1) composition in each complex essentially localized on the ligand (over 95%)

Solvatochromism of the Complexes 1–4

The absorption peaks of the complexes **1–4** are almost same in different solvents (Table 1). This suggests that the polarity of the solvent has very little influence on the ground state energy level of the complexes. However variation in the emission peak of the complexes **1–6** was observed in different solvents. The representative spectra of complex $[\text{Ir}(\text{dmpti})_2(\text{acac})]$ **1** is shown in Fig. 3. The emission peak of complexes **1–4** are around 430 nm in *n*-hexane (non-polar), 512 nm in ethanol (polar protic solvent), 505 nm in CH_2Cl_2 (medium polarity) and 528 nm in acetonitrile (a strongly polar aprotic solvent). The peak shift may be due to the stronger interaction between the solvents and the excited state molecules. The excited state of all iridium complexes are more stabilized in polar solvents than in non-polar solvents which leads to red shift of emission with increasing solvent polarity [27] (Fig. 4). The photo luminescent peak of solid state (representative spectrum of complex **1** is shown in Fig. 3) of all complexes are almost similar to that of emission in non-polar solvent (*n*-hexane) which shows that there is very little or no influence of molecular interaction on the excited state of iridium complexes in the solid state [27].

Mixing of Excited States (LC and MLCT)

Phosphorescence of mononuclear metal complexes originates from the ligand-centered excited state, metal-centered excited state and MLCT excited state. For the cyclo-metallated iridium (III) complexes, the wave function of the excited triplet state Φ_T , responsible for the phosphorescence is expressed as,

$$\Phi_T = a\Phi_T(\pi - \pi^*) + b\Phi_T(\text{MLCT}) \quad (2)$$

where ‘a’ and ‘b’ are the normalized co-efficients, $\Phi_T(\pi - \pi^*)$ and $\Phi_T(\text{MLCT})$ are the wave function of ${}^3(\pi - \pi^*)$ and ${}^3(\text{MLCT})$ excited states, respectively. For these iridium complexes, the wave function of the triplet state (Φ_T) responsible for the phosphorescence and Eq. 2 implies that the excited triplet state of these iridium complexes are mixture of $\Phi_T(\pi - \pi^*)$ and $\Phi_T(\text{MLCT})$ [28]. The triplet state is attributed to dominantly ${}^3\pi - \pi^*$ excited state when $a > b$ and dominantly ${}^3\text{MLCT}$ excited state when $b > a$.

According to the previous report [12] phosphorescence spectra from the ligand-centered ${}^3\pi - \pi^*$ state display vibronic progressions while those from ${}^3\text{MLCT}$ state are broad and featureless. The phosphorescence spectra of these complexes (**1–4**) obtained at 298 K show significant broad shape and also vibronic fine structure. The luminescence spectra of complexes **1** and **3** reveal that broad shape of the luminescence spectra whereas the vibration pattern of the photoluminescence spectra were observed for the complexes **2** and **4**. Complexes **1** and **3** have excited state with large contribution of ${}^3\text{MLCT}$ whereas complexes **2** and **4** have excited state with large contribution of ${}^3(\pi - \pi^*)$.

Table 1 Photoluminescence spectral data of various solvents and solid emission spectra of complexes **1–6**

Solvent	Absorption ^a (λ , nm) ($\log \varepsilon$)				Emission ^b (λ , nm)			
	1	2	3	4	1	2	3	4
<i>n</i> -Hexane	251 (3.98)	257 (3.98)	260 (3.94)	275 (3.98)	431	440	502	504
	329 (3.68)	330 (3.85)	325 (3.74)	328 (3.85)				
	385 (3.33)	378 (3.52)	382 (3.49)	371 (3.71)				
	—	—	425 (3.35)	394 (3.32)				
1,4-dioxan	290 (3.99)	277 (3.95)	272 (3.94)	276 (3.99)	444	445	455	458
	330 (3.70)	293 (3.78)	320 (3.78)	313 (3.85)				
	385 (3.29)	326 (3.60)	373 (3.60)	374 (3.61)				
	—	378 (3.36)	—	—				
Benzene	279 (3.91)	275 (3.91)	280 (3.95)	275 (3.92)	430	428	450	454
	328 (3.64)	331 (3.84)	354 (3.88)	337 (3.74)				
	382 (3.37)	382 (3.56)	390 (3.70)	370 (3.50)				
	—	408 (3.35)	417 (3.50)	393 (3.23)				
Chloroform	255 (3.91)	267 (3.98)	243 (3.98)	241 (3.94)	489	491	498	500
	328 (3.71)	333 (3.76)	269 (3.85)	274 (3.78)				
	385 (3.44)	379 (3.44)	378 (3.69)	339 (3.51)				
	—	—	411 (3.45)	381 (3.23)				
Ethyl acetate	274 (3.91)	276 (3.96)	275 (3.91)	277 (3.98)	476	487	500	510
	328 (3.71)	339 (3.76)	350 (3.78)	322 (3.94)				
	383 (3.44)	376 (3.53)	383 (3.62)	351 (3.78)				
	—	—	416 (3.37)	396 (3.61)				
Dichloromethane	276 (3.96)	270 (3.96)	230 (4.09)	256 (3.94)	505	507	510	514
	328 (3.63)	337 (3.76)	274 (3.97)	330 (3.85)				
	383 (3.35)	376 (3.51)	355 (3.35)	376 (3.72)				
	—	—	415 (3.06)	408 (3.51)				
1-Butanol	256 (3.86)	263 (3.96)	224 (3.96)	281 (3.94)	510	515	518	520
	329 (3.39)	327 (3.86)	267 (3.89)	346 (3.85)				
	382 (3.01)	382 (3.70)	336 (3.74)	390 (3.77)				
	—	398 (3.47)	398 (3.49)	406 (3.61)				
Ethanol	256 (3.95)	263 (3.95)	275 (3.95)	273 (3.98)	512	518	520	525
	332 (3.65)	285 (3.77)	350 (3.75)	336 (3.85)				
	385 (3.49)	330 (3.59)	387 (3.51)	380 (3.77)				
	—	376 (3.41)	410 (3.29)	403 (3.61)				
Methanol	257 (3.91)	256 (3.96)	274 (3.90)	275 (3.98)	515	520	522	528
	328 (3.65)	330 (3.83)	330 (3.78)	355 (3.88)				
	388 (3.47)	381 (3.59)	380 (3.67)	385 (3.72)				
	—	—	404 (3.44)	402 (3.51)				
Acetonitrile	260 (3.95)	266 (3.94)	276 (3.78)	273 (3.98)	528	539	540	552
	331 (3.74)	314 (3.72)	345 (3.69)	332 (3.88)				
	382 (3.49)	378 (3.42)	386 (3.68)	386 (3.72)				
	—	—	415 (3.47)	404 (3.61)				
Solid emission spectra					431.7	441	501	503.8

^a UV-vis absorption measured in solution concentration = 1×10^{-5} M^b Photoluminescence measured in solution concentration = 1×10^{-4} M

In addition to $^3\text{MLCT}$ absorption bands with high intensity, strong spin-orbit coupling in iridium (III) complexes leads to efficient phosphorescence in these complexes. The absolute PL quantum yields were measured by comparing fluorescence intensities (integrated areas) of a

standard sample (Coumarin 46) and the unknown sample according to the following Eq. 3:

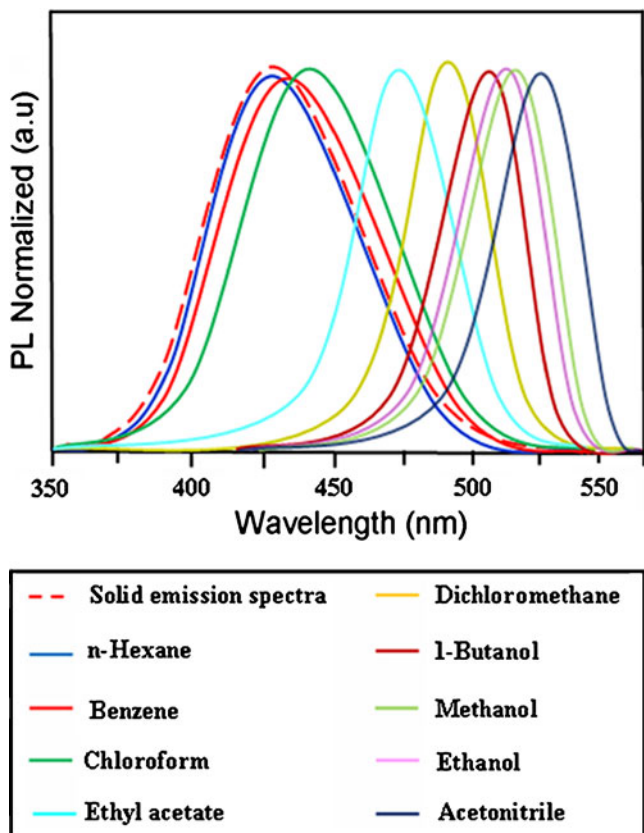
$$\Phi_{\text{unk}} = \Phi_{\text{std}} \left(\frac{I_{\text{unk}}}{I_{\text{std}}} \right) \left(\frac{A_{\text{std}}}{A_{\text{unk}}} \right) \left(\frac{\eta_{\text{unk}}}{\eta_{\text{std}}} \right)^2 \quad (3)$$

Table 2 DFT calculated% composition of selected frontier orbitals of **1** and **2** expressed in component fragments

Complex	Components	HOMO-1 (eV)	HOMO (eV)	LUMO (eV)	LUMO+1 (eV)
Ir(dmpti) ₂ (acac) (1)	Ir	10.3	15.8	7.9	0.9
	ligand	89.7	84.2	92.1	99.1
Ir(fpdmpti) ₂ (acac) (2)	Ir	5.9	12.6	7.1	5.0
	ligand	94.1	87.4	92.9	95.0

where Φ_{unk} is the fluorescence quantum yield of the sample, Φ_{std} is the fluorescence quantum yield of the standard; I_{unk} and I_{std} are the integrated emission intensities of the sample and the standard, respectively. A_{unk} , and A_{std} are the absorbances of the sample and the standard at the excitation wavelength, respectively. η_{unk} and η_{std} are the indexes of refraction of the sample and standard solutions. The main decay route of the excited state of these complexes (**1–4**) and their radiative and non-radiative decay (Table 3) are studied in detail (Fig. 5a). The radiative (k_r) and non-radiative (k_{nr}) rate constants are calculated by,

$$k_r = \Phi_p / \tau \quad (4)$$

**Fig. 3** The solid state and the solvatochromic emission spectra of the complex **1**

$$k_{\text{nr}} = 1/\tau - \Phi_p / \tau \quad (5)$$

$$\tau = (k_r + k_{\text{nr}})^{-1} \quad (6)$$

where k_r and k_{nr} are the radiative and non-radiative deactivation, τ_f is the life time of the S_1 excited state. The low quantum yields could be explained by non-radiative paths to the low-lying $n-\pi^*$ states of the nitrogen atoms. All these complexes (**1–4**) exhibit appreciable phosphorescence quantum yields at room temperature under nitrogen condition (Fig. 5b). These values appear to be high for (fpdmpti)₂Ir(acac) (**4**) complex [29]. Moreover, radiative lifetime of these complexes fall in the range of 1.4–2.3 μ s. Among these complexes, a significant feature of the highly emitting (fpdmpti)₂Ir(acac) (**4**) has short triplet excited state lifetime which is 1.4 μ s.

From the viewpoint of the relationship between maximum emission peak wavelength of photoluminescent spectra and decay rate constants, two trends are evident for the iridium complexes **1–4**. The radiative rate constant (k_r) increases with increase in the red shift (Fig. 5c) however the non-radiative decay rate constant (k_{nr}) does not show monotonous change i.e., nearly same for all complexes [29].

Description of the Structure of Ir(dmpti)₂(acac) (**5**)

In continuation of our previous work [20], the crystal structure of the complex, Ir(dmpti)₂(acac) **5** [20] is represented with an ORTEP diagram in Fig. 6 and selected bond lengths and bond angles are presented in Table 4. All these complexes exhibits an octahedral geometry around metal iridium and prefers *cis*-C,C and *trans*-N,N chelate disposition instead of *trans*-C,C and *trans*-N,N chelate. Electron rich phenyl rings normally exhibit very strong influence and *trans* effect. Therefore, the *trans*-C,C arrangement is expected to be thermodynamically higher in energy and the kinetically more labile [30]. This well known phenomenon has been referred to as “transphobia” [31]. The Ir–C bonds of the complex **5**, i.e. $\text{Ir}-\text{C}_{\text{av}}=1.998 \text{\AA}$ was found to be shorter than Ir–N bonds i.e., $\text{Ir}-\text{N}_{\text{av}}=2.055 \text{\AA}$. The Ir–O bond length [2.153 \AA] is longer than the mean Ir–O bond length (2.088 \AA) reported [32–34] and these observations reflect the *trans* influence of the phenyl

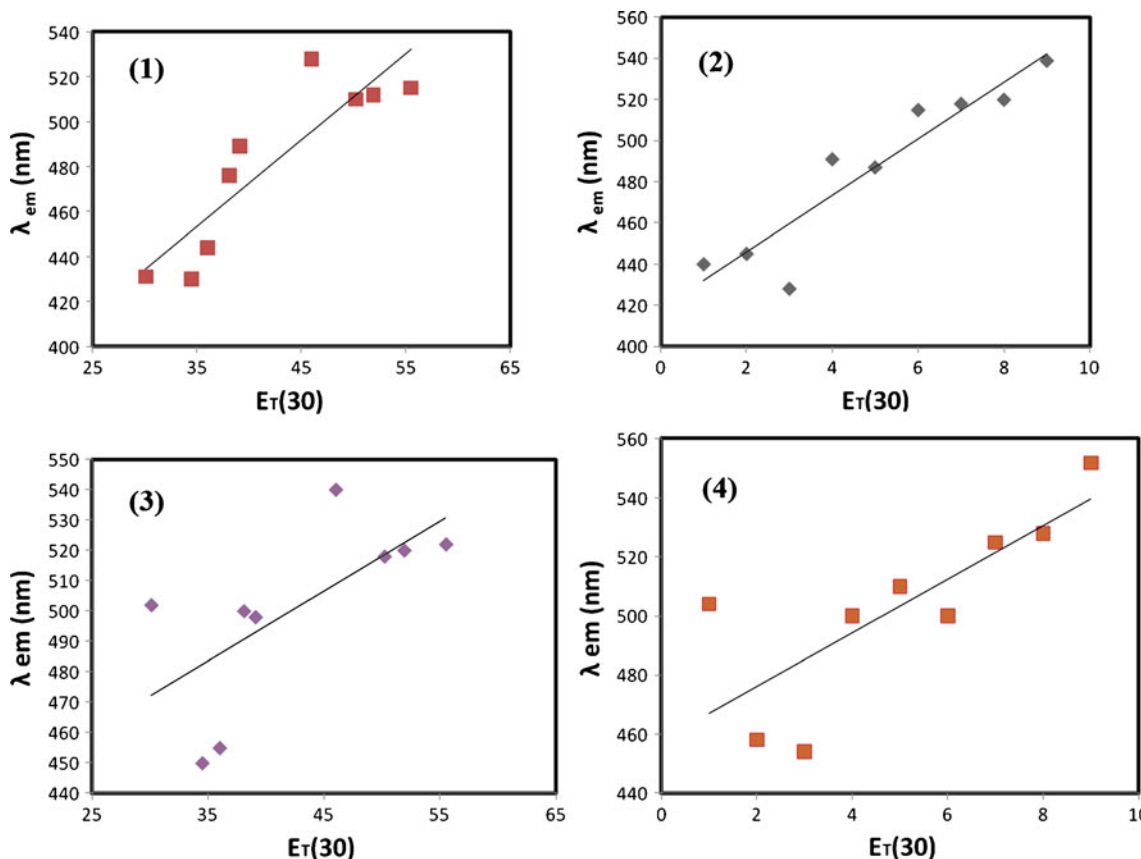


Fig. 4 Plot of λ_{em} versus $E_T(30)$

groups. All other bond lengths and bond angles are analogous to the similar type of complexes.

Electrochemistry

The electrochemical properties of the cyclometalated iridium complexes were examined by cyclic voltammetry. The redox potentials were measured relative to an internal ferrocene reference ($Cp_2Fe/Cp_2Fe^+=0.45$ V versus SCE in CH_2Cl_2 solvent) [35, 36] are given in Table 5. As revealed previously [37, 38] the reductions occur primarily on the more electron accepting heterocyclic portion of the cyclometalated 2-arylimidazole ligands LUMO contribution) whereas the oxidation process is generally considered to largely involve the Ir-phenyl centre (HOMO contribution).

The energies of the highest occupied molecular orbital (HOMO) and lowest unoccupied molecular orbital (LUMO) were calculated using the following Eqs. 7 and 8 and the calculated values are given in Table 5.

$$E_{\text{HOMO}} = 4.4 + E_{(\text{onset})} \quad (7)$$

$$E_{\text{LUMO}} = E_{\text{HOMO}} - 1239/\lambda_{\text{abs}} \quad (8)$$

The iridium complexes show reversible oxidation behaviour and these complexes exhibit HOMO levels ranging of 5.15–5.36 eV. The HOMO level of complexes 3 and 4 are higher than those reported for other iridium complexes [5.2 eV for $\text{Ir}(\text{ppy})_2(\text{acac})$ and 5.16 eV for $\text{Ir}(\text{btp})_2(\text{acac})$]

Table 3 Photophysical properties of iridium complexes 1–5

^a UV-vis absorption measured in CH_2Cl_2 solution, concentration= 1×10^{-5} M. ^b Photoluminescence measured in CH_2Cl_2 solution, concentration= 1×10^{-4} M

Complex	Quantum yield (φ)	Lifetime (μs) 298 K	k_r (μs^{-1})	k_{nr} (μs^{-1})
$\text{Ir}(\text{dmpti})_2(\text{acac})$ (1)	0.29	2.2	0.13	0.32
$\text{Ir}(\text{fpdmti})_2(\text{acac})$ (2)	0.32	2.0	0.16	0.34
$\text{Ir}(\text{dmdmppi})_2(\text{acac})$ (3)	0.42	1.6	0.26	0.36
$\text{Ir}(\text{fpdmdmppi})_2(\text{acac})$ (4)	0.56	1.4	0.40	0.31
$\text{Ir}(\text{dmdpi})_2(\text{acac})$ (5) [20]	0.08	2.3	0.03	0.40

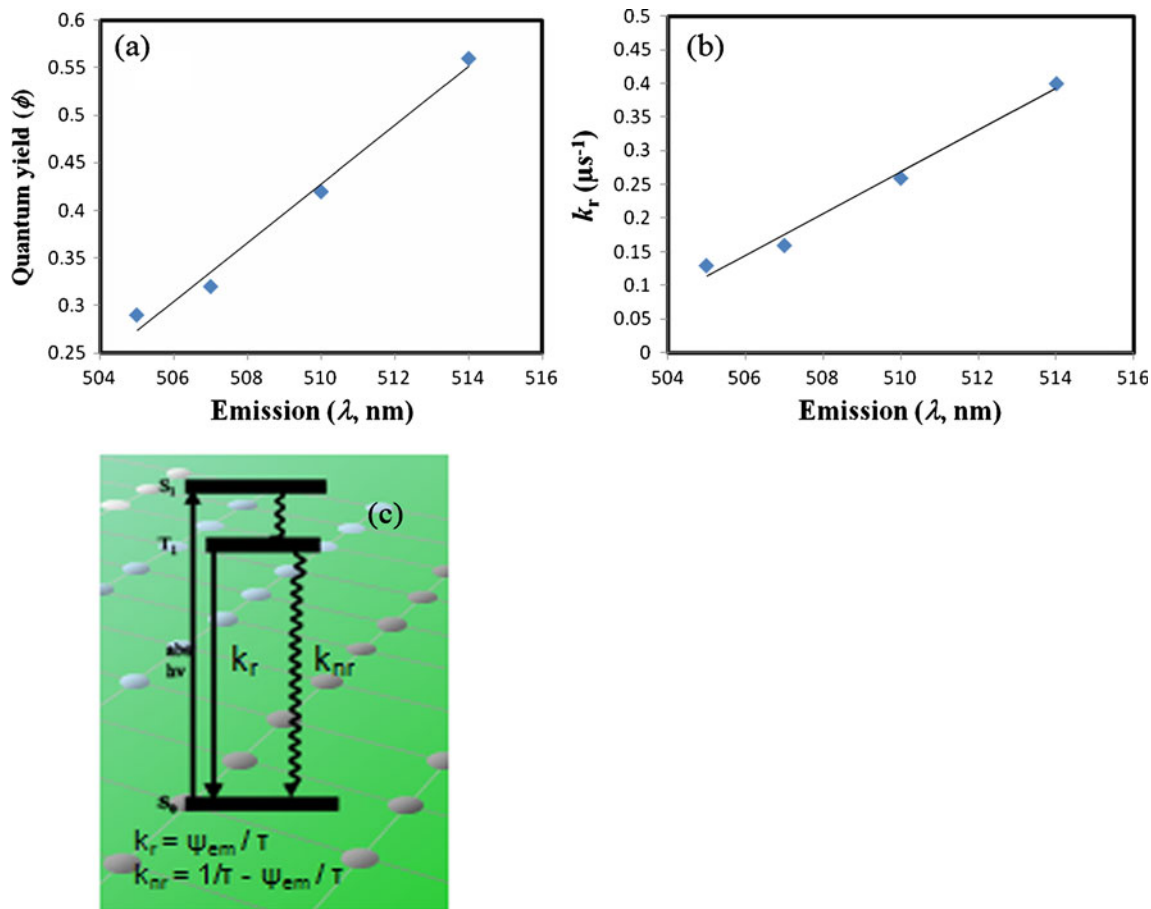


Fig. 5 **a** Plot of λ_{emi} versus Quantum yield. **b** Plot of λ_{emi} versus k_r . **c** Pathway of k_r and k_{nr}

[38]. The LUMO energies were calculated based on the HOMO energies and the lowest-energy absorption edges of the UV-vis absorption spectra [20, 36]. The calculated energy gap ($E_g = \text{HOMO-LUMO}$) for complexes **1** and **2** are minimum whereas complexes **(3)** and **(4)** exhibit

maximum energy gap (Fig. 7). These results reveal that the mono-methyl substituted complexes **1** and **2** show emission with the shorter wavelength [505 (**1**), 507 (**2**)] (minimum E_g) whereas dimethyl substituted complexes [$\text{Ir}(dmdmppi)_2(acac)$ (**3**) and $\text{Ir}(fpdmppi)_2(acac)$ (**4**)] (maximum E_g) exhibit

Fig. 6 ORTEP diagram for complex (**5**)

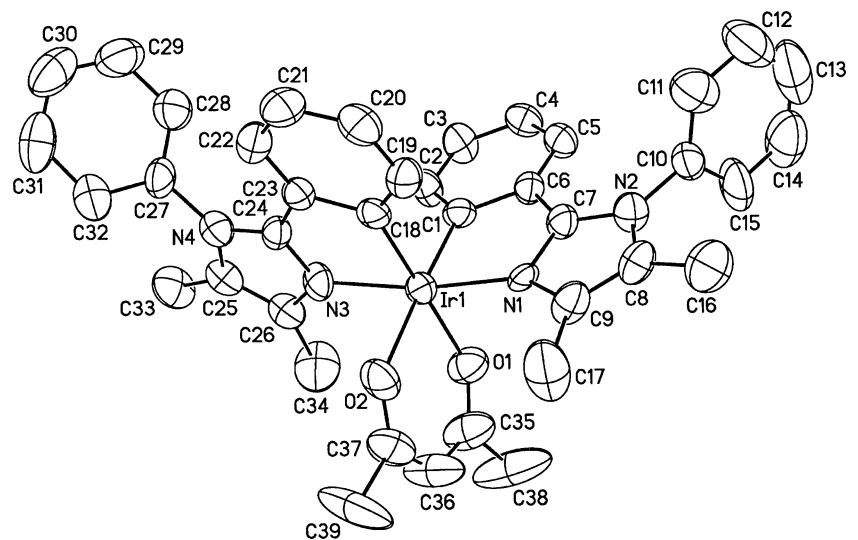


Table 4 Selected bond distances [Å] for $(\text{Ir}(\text{dmdpi})_2(\text{acac})$ 5

Complex	Atom (1)–Atom(2)	Distance [Å]	Average distance [Å]	Atom (1) – Atom(2) – Atom(3) (°)	Bond angle (°)
				C1-Ir1-C18	92.5 (93.1)
	Ir(1)-N(1)	2.012 (2.053)		C1-Ir1-N1	81.0 (82.6)
				C18-Ir1-N1	93.5 (94.2)
			Ir-N _{av} =2.055 (2.077)	N3-Ir1-N1	171.0 (171)
	Ir(1)-N(3)	2.089 (2.100)		C1-Ir1-O1	89.2 (90.1)
				C1-Ir1-O1	86.1 (90.0)
				N3-Ir1-O1	101.0 (103.2)
	Ir(1)-C(1)	1.994 (2.000)		C1-Ir1-O2	176.8 (178.0)
				C18-Ir1-O2	90.7 (92.6)
$\text{Ir}(\text{dmdpi})_2(\text{acac})$, 5			Ir-C _{av} =1.998 (2.004)	N1-Ir1-O2	176.8 (178.0)
	Ir(1)-C(18)	2.002 (2.008)		N3-Ir1-O2	87.4 (89.2)
				O1-Ir1-O2	87.6 (89.5)
				N1-C7-C6	117.4 (119.0)
	Ir(1)-O(1)	2.151 (2.162)		N4-C24-C23	110.1 (114.2)
			Ir-O _{av} =2.153 (2.161)	C7-Ir1-N1	113.8 (115.6)
				N1-C9-C17	120.1 (122.3)
	Ir(1)-O(2)	2.154 (2.160)		O2-C36-C38	113.3 (115.0)
				O1-C35-C37	126.5 (127.8)

Values in the parenthesis are calculated theoretically

emission with maximum wavelength [510 (**3**) and 514 nm (**4**)]. From the energy gap values it was concluded that all the reported dopants are green emitters (Fig. 8). Substituent effect of the d orbital (t_{2g}) stabilization of iridium metal through the carbon atom-iridium bonding and this identifies with the inductive effect of the substituents. Therefore, the HOMO stability and the emission energy gap are controlled by the nature and number of substituents and its inductive influence on the aromatic ring.

Effect of Substituent in the Phenyl Ring on HOMO

In the present study iridium complexes **1–4** have electron releasing methyl substituents on the phenyl ring attached to the nitrogen atom N(1) of the 2-arylimidazole ligand and electron withdrawing substituent (i.e., fluorine) on the phenyl ring attached to the carbon atom [C(2)] of the imidazole ligand (**2** and **4**). It is obvious that the HOMO level of complexes **1–4** is strongly affected by the number

of methyl substituent on the phenyl ring attached to the nitrogen atom of the imidazole moiety (Table 5). Comparisons of HOMO values of the iridium complexes reveal that the HOMO values are higher for complexes **3** and **4** than complexes **1** and **2**. This may be due to the additional electronic effect exerted by substituent causes stabilization of iridium complexes through the carbon atom-iridium bonding. Therefore, the HOMO stability and the emission energy gap are controlled by the number of substituents and its inductive influence on the aromatic ring [29].

Theoretical Approaches

Mixing of Excited States (LC and MLCT)

Calculations were performed using density functional theory (DFT) as implemented in the Gaussian-03 program [23]. The geometry optimization was carried out by B3LYP

Table 5 Cyclic Voltammetry data of complexes **1–6**

Complex	$E_{\text{(onset)}} (\text{V})$	HOMO (eV)	LUMO ^a (eV)	E_g (eV)
$\text{Ir}(\text{dmpti})_2(\text{acac})$ (1)	0.35	-5.15	-2.80	2.35
$\text{Ir}(\text{fpdmti})_2(\text{acac})$ (2)	0.41	-5.21	-2.91	2.30
$\text{Ir}(\text{dmdmppi})_2(\text{acac})$ (3)	0.49	-5.29	-3.09	2.22
$\text{Ir}(\text{fpdmdmppi})_2(\text{acac})$ (4)	0.56	-5.36	-3.24	2.12
$\text{Ir}(\text{dmdpi})_2(\text{acac})$ 5	0.20	-5.02	-2.52	2.50

^a Measurement was carried out in CH_2Cl_2 solution, concentration= 1×10^{-3} M

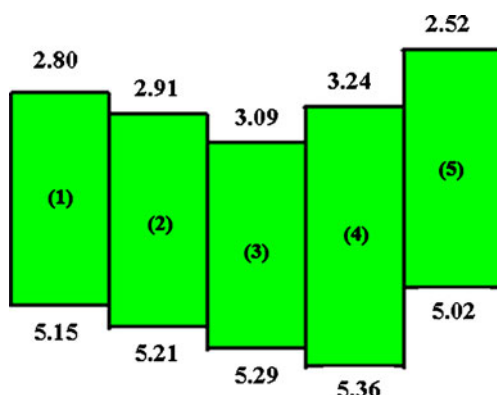


Fig. 7 HOMO-LUMO energy levels of the complexes 1–5

level using LANL2Z [24] basis set. The well known iridium complex $\text{Ir}(\text{ppy})_3$ was used as a reference that had $^3\text{MLCT}$ dominant lowest excited state [29] for which the calculated Mulliken charge difference on iridium atom between the ground state and the lowest triplet excited state was 0.45. The calculated Mulliken charges are 0.34 for $\text{Ir}(\text{fpdmpti})_2(\text{acac})$ (2) and 0.42 for $\text{Ir}(\text{dmpti})_2(\text{acac})$ (1) and this result strongly supports that $^3\pi-\pi^*$ is dominant for complex $\text{Ir}(\text{fpdmpti})_2(\text{acac})$ (2) owing to small reduction of Mulliken charge on iridium when compared with $\text{Ir}(\text{ppy})_3$ and $^3\text{MLCT}$ is dominant for complex $\text{Ir}(\text{dmpti})_2(\text{acac})$ (1) [23] owing to close to the value of $\text{Ir}(\text{ppy})_3$.

HOMO-LUMO Orbitals of $\text{Ir}(\text{dmpti})_2(\text{acac})$ (1)

The DFT calculations suggest that the highest occupied molecular orbital (HOMO) of these complexes are mainly localized on the phenyl rings of the 2-arylimidazole ligand and iridium center. On the contrary, the lowest unoccupied molecular orbital (LUMO) is localized on the imidazole

ring. The orbital picture predicts that variation in the electronic properties of the ligands should have an effect on the energy of the excited state and thereby confirmed the existence of remarkable photoinduced charge transfer properties [39].

Colour Tuning Based on DFT Calculations

On the basis of DFT calculation [23], the HOMO is localized on the imidazole ring and iridium center and LUMO is localized on the imidazole ring. Therefore it is decided to substitute the electron withdrawing substituent (i.e., fluoro) at *para* position of the phenyl ring attached to the carbon C (2) of the imidazole ring to stabilize LUMO energy and electron releasing substituent in the phenyl ring attached to the nitrogen N(1) of the imidazole ring for color tuning. From the emission peaks (Table 1) it was concluded that increasing the number of methyl substituent on the aldehydic part would cause a larger red shift in the emission spectra and it turns out that this expectation correlates well with the emission data [25].

Conclusions

We have synthesized a series of Ir(III) complex dopants using various substituted imidazole ligands. These complexes exhibit different quantum efficiencies in solution depending upon the nature of substituents. The wavelength can be tuned to greater extent depending upon the substituents in the ligand. Some of the complexes discussed here showed $^3\text{MLCT}$ predominant mixing states for their lowest excited triplet states. But the degree of mixing between $^3\text{MLCT}$ and $^3\pi-\pi^*$ states of the excited states varied. The experimental reports are supported by DFT calculation and effort towards the development of RGB colour complexes using different substituents are currently underway and investigation of device studies for these Iridium complexes are also currently in progress.

Acknowledgements One of the authors Dr. J. Jayabharathi, Associate professor of Chemistry, Annamalai University is thankful to University Grants Commission (F. No. 36-21/2008 (SR)), Department of Science and Technology [No. SR/S1/IC-07/2007] for providing fund to this research work and Prof. C.H. Cheng, Chairman, National Science Council, National Tsing Hua University for my post-doctoral research work.

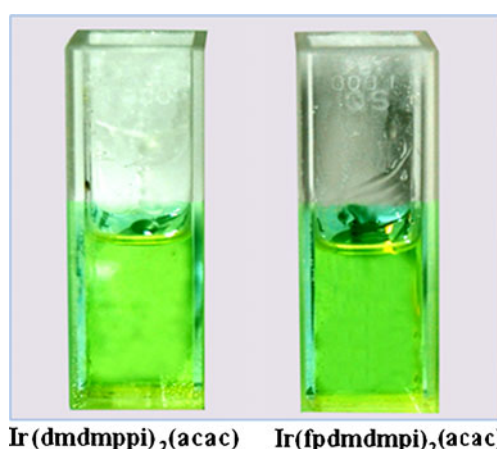


Fig. 8 Solution color of the photoluminescence for complexes 3 and 4

References

- Baldo MA, O'Brien DF, You Y, Shoustikov A, Thompson ME, Forrest SR (1988) Highly efficient phosphorescent emission from organic electroluminescent devices. *Nature* 395:151–154

2. Baldo MA, Thompson ME, Forrest SR (1999) Phosphorescent materials for application to organic light emitting devices. *Pure Appl Chem* 71:2095–2106
3. Ionkin AS, Marshall WJ, Wang Y (2005) Syntheses, structural characterization, and first electroluminescent properties of mono-cyclometalated platinum(II) complexes with greater than classical π - π stacking and Pt–Pt distances. *Organometallics* 24:619–627
4. Furuta PT, Deng L, Garon S, Thompson ME, Frechet JMJ (2004) Platinum-functionalized random copolymers for use in solution-processible, efficient, near-white organic light-emitting diodes. *J Am Chem Soc* 126:15388–15389
5. Sotoyama W, Satoh T, Sawatari N, Inoue H (2005) Efficient organic light-emitting diodes with phosphorescent platinum complexes containing $N\wedge N$ -coordinating tridentate ligand. *Appl Phys Lett* 88(153505):1–3
6. Baldo MA, Lamansky S, Burrows PE, Thompson ME, Forrest SR (1999) Very high-efficiency green organic light-emitting devices based on electrophosphorescence. *Appl Phys Lett* 75:4–6
7. Idle N, Matusue N, Kobayashi T, Naito H (2006) Photoluminescence properties of *facial*- and *meridional*-Ir(ppy)₃ thin films. *Thin Solid Films* 509:164–167
8. Adachi C, Baldo MA, Forrest SR, Lamansky S, Thompson ME, Kwong RC (2001) High-efficiency red electrophosphorescence devices. *Appl Phys Lett* 78:1622–1624
9. Chen HY, Chi Y, Liu CS, Yu JK, Cheng YM, Chen KS, Chou PT, Peng SM, Lee GH, Carty AJ, Yeh SJ, Chen CT (2005) Rational color tuning and luminescent properties of functionalized boron-containing 2-pyridyl pyrrolide complexes. *Adv Funct Mater* 15:567–574
10. Lowry MS, Bernhard S (2006) Synthetically tailored excited states: phosphorescent, cyclometalated Iridium(III) complexes and their applications. *Chem Eur J* 12:7970–7977
11. Hwang EM, Chen HY, Chen PS, Liu CS, Shu CF, Wu EL, Chou PT, Peng SM, Lee GH (2005) Iridium(III) complexes with orthometalated quinoxaline ligands: subtle tuning of emission to the saturated red color. *Inorg Chem* 44:1344–1353
12. Lamansky S, Djurovich P, Murphy D, Abdel-Razzaq F, Lee HF, Adachi C, Burrows PE, Forrest SR, Thompson ME (2001) Highly phosphorescent bis-cyclometalated iridium complexes: synthesis, photophysical characterization and use in organic light emitting diodes. *J Am Chem Soc* 123:4304–4312
13. Thompson ME, Lamansky S, Djurovich P, Murphy D, Abdel-Razzaq F, Kwong R, Forrest SR, Baldo MA, Burrows PE. US Patent 20020034656A1
14. Brooks J, Babayan Y, Lamansky S, Djurovich PI, Tsby I, Bau R, Thompson ME (2002) Synthesis and characterization of phosphorescent cyclometalated platinum complexes. *Inorg Chem* 41:3055–3066
15. Grushin VV, Herron N, LeCloux DD, Marshall WJ, Petrov VA, Wang Y (2001) New, efficient electroluminescent materials based on organometallic Ir complexes. *Chem Commun* 16:1494–1495
16. Chang WC, Hu AT, Duan JP, Rayabarapu DK, Cheng CH (2004) Color tunable phosphorescent light-emitting diodes based on iridium complexes with substituted 2-phenylbenzothiazoles as the cyclometalated ligands. *J Organomet Chem* 689:4882–4888
17. Colombo MG, Hauser A, Gudel HU (1993) Evidence for strong mixing between the LC and MLCT excited states in bis(2-phenylpyridinato-C₂, N')(2, 2'-bipyridine)iridium(III). *Inorg Chem* 32:3088–3092
18. Jayabharathi J, Thanikachalam V, Saravanan K, Srinivasan N (2010) Iridium(III) complexes with orthometalated imidazole ligands subtle turning of emission to the saturated green colour. *J Fluoresc.* doi:10.1007/s10895-010-0737-7
19. Saravanan K, Srinivasan N, Thanikachalam V, Jayabharathi J (2010) Synthesis and photophysics of some novel imidazole derivatives used as sensitive fluorescent chemisensors. *J Fluoresc.* doi:10.1007/s10895-010-0690-5
20. Jayabharathi J*, Thanikachalam V, Srinivasan N, Saravanan K (2010) Synthesis, structure, luminescent and intramolecular proton transfer in some imidazole derivatives. *J Fluoresc.* (doi:10.1007/s10895-010-0747-5)
21. Jayabharathi J, Thanikachalam V, Saravanan K (2009) Effect of substituents on the photoluminescence performance of Ir(III) complexes: synthesis, electrochemistry and photophysical properties. *J Photochem Photobiol A* 208:13–20
22. Yoshinobu G, Noriko H, Motoyoshi Y (1970) Studies on azole compounds. II. Reaction of oxazole N-oxides with phenyllisocyanate to give imidazole derivatives. *Chem Pharm Bull* 18:2000–2008
23. Nonoyama M (1974) Benzo(*h*)quinolin-10-yl-N Iridium(III) complexes. *Bull Chem Soc Jpn* 47:767–768
24. Schaffner-Hamann C, Zelewsky A, Barbieri A, Barigelli F, Muller F, Riehl JP, Neels A (2004) Diastereoselective formation of chiral tris-cyclometalated Iridium (III) complexes: characterization and photophysical properties. *J Am Chem Soc* 126:9339–9348
25. Zhang L, Li B, Shi L, Li W (2009) Synthesis, structures, and photophysical properties of fluorine-functionalized yellow-emitting iridium complexes. *Opt Mater* 31:905–911
26. Lamansky S, Djurovich P, Murphy D, Abdel-Razzaq F, Kwong R, Tsby I, Bortz M, Mui B, Bau R, Thompson ME (2001) Synthesis and characterization of phosphorescent cyclometalated iridium complexes. *Inorg Chem* 40:1704–1711
27. Mi B-X, Wang PF, Liu M-W, Kwong H-L, Wong N-B, Lee CS, Lee ST (2003) Thermally stable hole-transporting material for organic light emitting diode: an isoindole derivative. *Chem Mater* 15:3148–3151
28. Djurovich P, Murphy D, Abdel-Razzag F, Kwong R, Tsby I, Bortz M, Mui B, Bau R, Thompson ME (2001) Synthesis and characterization of phosphorescent cyclometalated iridium complexes. *Inorg Chem* 40:1704–1711
29. Okada S, Okinaka K, Iwakawa H, Furugori M, Hashimoto M, Mukaide T, Kamatani J, Igawa S, Tsuboyama A, Takiguchi T, Ueno K (2005) Substituent effect of Iridium complexes for highly efficient red OLEDs. *Dalton Trans* 15:83–1590
30. Vicente J, Arcas A, Bautista D, De Arellano MCR (2002) Mono- and di-nuclear complexes of ortho-palladated and -platinated 4, 4'-dimethylazobenzene with bis(diphenylphosphino)methane. More data on transphobia. *J Organomet Chem* 663:164–172
31. Hwang GT, Son HS, Ku JK, Kim BH (2003) Synthesis and photophysical studies of bis-enediynes as tunable fluorophores. *J Am Chem Soc* 125:11241–11248
32. Urban R, Kramer R, Mihan S, Polborn K, Wagner B, Beck W (1996) Metal complexes of biologically important ligands, LXXXVII-amino carboxylate complexes of palladium(II), iridium(III) and ruthenium(II) from chloro-bridged orthometalated metal compounds and [(OC)3Ru(Cl)(-Cl)]₂. *J Organomet Chem* 517:191–200
33. Liu Z, Guan M, Bian Z, Nie D, Gong Z, Li Z, Huang C (2006) Red phosphorescent iridium complex containing carbazole-functionalized β -diketonate for highly efficient nondoped organic light emitting diodes. *Adv Funct Mater* 16:1441–1448
34. Gange RR, Koval CA, Lisenky GC (1980) Ferrocene as an internal standard for electrochemical measurements. *Inorg Chem* 19:2854–2855
35. Ranjan S, Lin SY, Hwang KC, Chi Y, Ching WL, Liu CS, Tao YT, Chien CH, Peng SM, Lee GH (2003) Realizing green phosphorescent light-emitting materials from rhenium(I) complexes. *Inorg Chem* 42:1248–1255

36. Hay PJ (2002) Theoretical studies of the ground and excited electronic states in cyclometalated phenylpyridine Ir(III) complexes using density functional theory. *J Phys Chem A* 106:1634–1641
37. Sudhakar M, Djurovich PI, Hogen-Esch TE, Thompson ME (2003) Phosphorescence quenching by conjugated polymers. *J Am Chem Soc* 125:7796–7797
38. Chen FC, He G, Yang Y (2003) Triplet exciton confinement in phosphorescent polymer light-emitting diodes. *Appl Phys Lett* 82:1006–1008
39. Cheng CC, Yu WS, Chou PT, Peng SM, Lee GH, Wu PC, Song YH, Chi Y (2003) Syntheses and remarkable photophysical properties of 5-(2-pyridyl)pyrazolate boron complexes: photoinduced electron transfer. *Chem Commun* 2628–2629